The equation of state of molybdenum at 1400 °C

Gregory H. Miller, Thomas J. Ahrens, and Edward M. Stolper
Division of Geological and Planetary Sciences, California Institute of Technology, Pasadena, California 91125

(Received 5 October 1987; accepted for publication 3 December 1987)

Shock compression data to 96 GPa for pure molybdenum, initially heated to 1400 °C, are presented. Finite strain analysis of the data gives a bulk modulus at 1400 °C, K_{0S}, of 244 ± 2 GPa and its pressure derivative, K'_{0S}, of 4. A fit of shock velocity to particle velocity gives the coefficients of $U_S = c_0 + sU_P$ to be $c_0 = 4.77 \pm 0.06$ km/s and $s = 1.43 \pm 0.05$. From the zero-pressure sound speed c_0, a bulk modulus of 232 ± 6 GPa is calculated which is consistent with extrapolation of ultrasonic elasticity measurements. The temperature derivative of the bulk modulus at zero pressure, $\partial K_{0S}/\partial T|_P$, is approximately −0.012 GPa/K. A thermodynamic model is used to show that the thermodynamic Grüneisen parameter is proportional to the density and independent of temperature. The Mie–Grüneisen equation of state adequately describes the high-temperature behavior of molybdenum under the present range of shock loading conditions.

I. INTRODUCTION

The equation of state (EOS) of molybdenum (Mo) at high pressures is being used as a calibration standard to relate absolute pressure-density data to diamond anvil compression data.[1] Both shock and particle velocity have been measured for Mo shocked with a nuclear explosive[2] to obtain Hugoniot data to 2.0 TPa. Mo is thus well calibrated along the room-temperature (or "principal") Hugoniot, yet theoretical arguments are necessary to extend the shock EOS to neighboring regions of P-V-T space. The present study is the first study of the absolute EOS of any metal at significantly high initial temperatures. A 1400 °C Mo Hugoniot has been measured which calibrates models for this P-V-T extrapolation.

One of the research efforts of the experimental geophysics group at Caltech is the study of molten silicates under shock loading conditions. These experiments, developed by Rigden, Ahrens, and Stolper,[3,4] employ a Mo sample assembly that both contains the sample at temperature in excess of 1400 °C and acts as a furnace by coupling to a radio frequency power source. A flyer plate, propelled by a gun, impacts the first surface of the heated Mo container, and the subsequent shock wave traverses the Mo driver plate, then the silicate sample, and finally the Mo cover. The transit time of the shock wave through the sample and cover combination is recorded with a rotating prism streak camera. A direct impedance match solution[5] for this composite sample assembly requires knowledge of the shock behavior of either the molten sample or the heated Mo. Since the former is the objective of these experiments, the latter must either be calculated or experimentally determined. Rigden and co-workers[3,4] calculated the high-temperature shock behavior of Mo from its known principal Hugoniot with a Mie–Grüneisen extension of the Birch–Murnaghan EOS.[6]

In order to verify these calculations, we undertook an experimental study of the dynamic loading properties of Mo at 1400 °C, the temperature to which Rigden and co-workers heated their molten anorthite-diopside eutectic composition. In addition to their direct relevance to our shock wave studies of molten silicates, our new results on hot Mo give more general insights into the high-temperature and pressure equations of state of metals.

II. EXPERIMENTAL PROCEDURE

Dynamic shock compression of hot Mo was achieved using the Caltech 40-mm powder gun.[5] The experimental procedure is similar to that used by Rigden and co-workers[3,4] for the shock measurements of the EOS of molten silicates.

Molybdenum of 99.95% purity, specification ABL-2 from Amac Specialty Metals, Cleveland, was used. The samples were machined from this polycrystalline stock into a single piece driver plate-sample combination as shown in Fig. 1. A 2-mm-thick, 45-mm-diam disk of Mo acts as the driver plate, and a 3.6-mm-thick, 13.5-mm-diam disk of Mo coaxial to the driver plate, is the sample.

The Mo samples were supported by a 6.4-mm-thick plate of fibrous Al_2O_3 ceramic at a distance of approximately

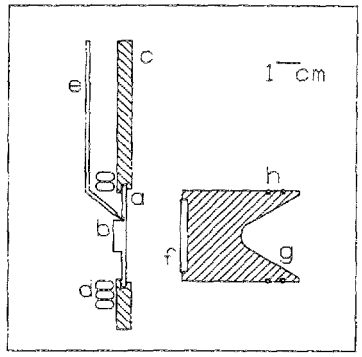

FIG. 1. Schematic cross section of the experimental setup. A molybdenum driver plate (a) and sample (b) are machined as a single piece. The sample is suspended in a fibrous Al_2O_3 ceramic plate (c) adjacent to a copper induction coil (d). Preheat temperatures are recorded by the 100% Pt—90% Pt 10% Rh thermocouple (e) which is pressed into the sample. A tungsten or 2024 aluminum flyer plate (f) is pressed into a Lexan projectile (g) with O-rings (h) to help retain the muzzle gasses.

 0021-8979/88/094469-07$02.40

TABLE I. Parameters used in data reduction.

	c_0(km/s)	s	ρ_0(Mg/m^3)
W	4.029[a]	1.237[a]	19.224[a]
2024 Al	5.328[a]	1.338[a]	2.785[a]
Mo	5.14[b]	1.22[b]	10.2201[c]

$$\Delta L/L_0 = 4.697\times10^{-6}(T-293) + 9.756\times10^{-10}(T-293)^2 + 9.403\times10^{-14}(T-293)^3$$

for Mo from 293 to 1545 K, $\pm$ 4%, and

$$\Delta L/L_0 = 7.60\times10^{-3} + 7.583\times10^{-6}(T-1545) + 1.329\times10^{-9}(T-1545)^2 + 1.149\times10^{-12}(T-1545)^3$$

for Mo from 1545 to 2800 K, $\pm$ 5%[d]

$\gamma_{0,\mathrm{Mo}} = 1.52$[e]

$$C_p = 34.139 - 4.4926\times10^{-3}T + 3.7012\times10^{-6}T^2 - \frac{1.5722\times10^2}{\sqrt{T}}\ \mathrm{J\ mol^{-1}\ K^{-1}}$$

for Mo from 298 to 1800 K[f]

[a] Reference 7.
[b] Reference 8.
[c] Reference 9.
[d] Reference 10.
[e] Reference 11.
[f] Reference 12.

1 mm from a three-turn water-cooled copper coil. This coil, attached to a 10-kW radio frequency source, acted as an induction heater. Temperatures in excess of 1800 °C could be achieved with this configuration. At 1400 °C, the temperature can be stabilized to within one half degree. A 100%Pt—90%Pt 10%Rh thermocouple was pressed into a well in the sample to record its preheating temperature. Light reflected from the free surface of the sample and driver was turned by a mirror in the tank to a port at the side of the tank. This reflected light was subsequently focused onto the slit of a continuous writing streak camera. This streak record was used to record the shock transit time within the sample. A xenon flash lamp operating at 10–15 kV was used to illuminate the sample during the experiment.

The flyer plates were 2.4-mm-thick, 32-mm-diam disks of either tungsten or 2024 aluminum mounted in a Lexan projectile. The velocity of the projectile was recorded with a double-exposure x-ray shadowgraph. The x-ray exposure occurred immediately prior to impact. As a backup device, the time taken for the projectile to cross the known distances between three lasers which cross the flight path is measured. Projectile velocities were between 1.5 and 2.5 km/s.

The measured quantities in our experiment are the sample and flyer plate density, initial sample temperature, the shock transit time in the sample, and the velocity of impact.

III. RESULTS AND DISCUSSION

The shock pressure P_H and sample density ρ_{HS} were calculated from the Rankine–Hugoniot equations for stress and mass conservation across the flyer plate-driver/sample interface. Sample thickness and initial density are not directly measured, but calculated from their measured room-temperature values, the sample preheat temperature, and the linear thermal expansion data in Table I. The shock states with their estimated rms errors are given in Table II.

Our analysis of these results is presented in parts. First, we demonstrate that our final shock states are solid and not liquid. Second, we determine the isentropic bulk modulus and its pressure derivative for Mo at 1400 °C with both a finite strain model and the shock EOS. Third, we compare our shock data with the theoretical predictions of the Mie–Grüneisen EOS and show that the Grüneisen parameter varies in proportion to density. Fourth and finally, we compare our data with elasticity measurements to discriminate between three possibile interpretations of our data.

A. Shock state: Solid versus liquid

The calculated melting temperature for Mo is at least 1000 K higher than the calculated shock temperatures of our experiments at a given shock pressure. Our final shock states therefore represent solid Mo in all cases.

The Rankine–Hugoniot equations can be used to determine the pressure (P), volume per unit mass (V), and internal energy per unit mass (E) along the Hugoniot. A constitutive relationship is necessary to relate these state variables to the temperature (T). The Mie–Grüneisen equation is a useful constitutive relationship for this purpose and has a strong theoretical foundation.[13]

The thermodynamic Grüneisen parameter, $\gamma \equiv -\partial \ln T/\partial \ln V|_s$, relates internal energy and pressure according to the Mie–Grüneisen equation, $\partial P/\partial E|_v = \gamma/V$. The Grüneisen parameter is assumed to be a function of volume according to

$$\frac{d\ln\gamma}{d\ln V} \equiv q, \tag{1}$$

where q is assumed to be constant, and it is further assumed that the temperature dependence of γ lies solely in the temperature dependence of the volume.

TABLE II. Experimental results.

Shot No.	Flyer	$\rho_{298\,\mathrm{K}}$ (Mg/m^3)	T_0 (K)	V_{imp} (km/s)	U_S (km/s)	U_P (km/s)	P_H (GPa)	ρ_H (Mg/m^3)	T_H[a] (K)
707	W	10.206 ± 0.002	1667	1.456 ± 0.007	5.960 ± 0.119	0.883 ± 0.008	52.3 ± 1.1	11.68 ± 0.05	1887 ± 532
716	W	10.206 ± 0.002	1673	1.527 ± 0.006	6.115 ± 0.047	0.919 ± 0.004	55.9 ± 0.5	11.70 ± 0.02	2602 ± 222
725	W	10.210 ± 0.002	1671	2.030 ± 0.010	6.516 ± 0.049	1.219 ± 0.009	79.0 ± 0.8	12.24 ± 0.03	3101 ± 367
736	2024 Al	10.207 ± 0.002	1674	1.995 ± 0.008	5.525 ± 0.041	0.538 ± 0.004	29.5 ± 0.3	11.02 ± 0.02	1864 ± 174
741	W	10.212 ± 0.002	1674	2.368 ± 0.008	6.788 ± 0.021	1.414 ± 0.006	95.6 ± 0.5	12.57 ± 0.02	3721 ± 253

[a] Temperatures calculated with $q = 1$.

Recognizing that $\partial E/\partial T|_v = C_v$, the heat capacity at constant volume, temperature, and pressure are related by $\partial T/\partial P|_v = V/(\gamma C_v)$. Integration of this equation along a path of constant volume requires a reference P-T point at the volume of interest. It is convenient to use the principal isentrope as a reference curve since pressure and temperature are readily calculated for any specified volume. The principal isentrope is a path of constant entropy which, like the principal Hugoniot, passes through the 1 bar, 20 °C point.

Along an isentrope, the temperature is readily calculated[14] from the definition of γ

$$T_S = T_0 \exp\{\gamma_0/q[1-(V/V_0)^q]\} \quad q \neq 0, \tag{2a}$$

$$T_S = T_0(V_0/V)^{\gamma_0}, \quad q = 0. \tag{2b}$$

where the subscript S denotes the isentropic state, and V_0, T_0, and γ_0 are the volume, temperature, and Grüneisen parameter at zero pressure, 25 °C, respectively.

Pressure along an isentrope may be calculated from the third-order Birch–Murnaghan equation

$$P_s = \tfrac{3}{2}K_{0S}\left[\left(\frac{V_0}{V}\right)^{7/3} - \left(\frac{V_0}{V}\right)^{5/3}\right]\left[1 - \frac{3}{4}(4 - K'_{0S}) \times\left[\left(\frac{V_0}{V}\right)^{2/3} - 1\right]\right], \tag{3}$$

where K_{0S} is the isentropic bulk modulus at zero pressure and K'_{0S} is its pressure derivative.

Using the isentrope as a reference curve, the temperature of a point on the Hugoniot, T_H, may be calculated from

$$T_H = T_S + [V_H(P_H - P_S)/\gamma C_V], \tag{4}$$

where the subscript H denotes a point on the Hugoniot. It has been assumed for simplicity (justification follows) that the heat capacity may be taken as a constant. The isentrope temperature T_S, pressure P_S, and the Grüneisen parameter γ in Eq. (4) are calculated at the Hugoniot volume V_H.

The shock temperatures achieved in our experiments were calculated with Eqs. (1)–(4) using values of V_H and P_H (Table II) calculated from the Rankine–Hugoniot equations. Specifically, the Grüneisen parameter is calculated at V_H with Eq. (1), and the isentrope pressure P_S, and temperature T_S are calculated using Eqs. (2) and (3) with $V = V_H$. The Hugoniot pressure P_H and volume V_H are used with these isentrope points in Eq. (4) to calculate the Hugoniot temperature T_H.

A general temperature-pressure relationship for the Hugoniot can be calculated in the same manner by using an appropriate constitutive relationship for P_H as a function of V_H. The Mie–Grüneisen formulation for this relationship is developed in a subsequent section of the discussion.

The melting point of Mo at high pressures may be estimated by Lindemann's rule, given by Gilvarry[15] as

$$\left.\frac{\partial \ln T}{\partial \ln V}\right|_M = 2(\tfrac{1}{3} - \gamma_D), \tag{5}$$

where the subscript M designates melting. γ_D is the Debye model for the Grüneisen parameter, $\gamma_D \equiv -d\ln\Theta_D/d\ln V$, where Θ_D is the Debye temperature. We evaluate Eq. (5) with the approximation that the Debye model Grüneisen parameter is equal to the thermodynamic Grüneisen parameter, which assumes that the Debye model is valid for Mo and that $T \gg \Theta_D$. The Debye temperature for Mo is 380 K,[16] and the melting temperature at zero pressure is 2893 K,[17] thus the latter assumption is valid. Because we are principally concerned with temperatures in excess of the Debye temperature, we make the additional assumption that $C_V = 3R$, where R is the gas constant. Combining Eqs. (1) and (5) with the assumption $\gamma \approx \gamma_D$ and integrating, we get the results

$$T_M = T_{0M}\left(\frac{V_M}{V_{0M}}\right)^{2/3} \exp\left(\frac{2\gamma_0(V_{0M}^q - V_M^q)}{qV_0^q}\right), \quad q \neq 0, \tag{6a}$$

$$T_M = T_{0M}\,(V_M/V_{0M})^{2(1/3-\gamma_0)}, \quad q = 0, \tag{6b}$$

where V_M amd T_M are the temperature and corresponding volume of the solid along the melting curve. $V_M = V_{0M}$ and $T_M = T_{0M}$ at the zero-pressure melting point. V_0 is the volume at which $\gamma = \gamma_0$.

The pressure P_M at which melting occurs for a particular T_M and V_M may again be calculated with the aid of the Mie–Grüneisen equation. Rearranging Eq. (4) and changing subscripts (M for H):

$$P_M = P_S + [\gamma C_V(T_M - T_S)/V_M]. \tag{7}$$

To evaluate Eq. (7), the isentrope points P_S and T_S and the Grüneisen parameter γ are calculated at $V = V_M$.

A check of the internal consistency of these calculations can be made by computing the melting temperature at zero pressure by simultaneous solution of Eq. (1)–(3), (6), and (7). The calculated temperature exceeds the known value by about 200 K when $q = 1$.

The shock temperatures, calculated with $q = 1$, are shown with the calculated melting curve for Mo in Fig. 2. The calculated melting curve for Mo exceeds the calculated experimental shock temperatures by over 1000 K in all cases. It is evident that our experimental points are well within the field of solid stability as judged by the Lindemann's rule calculations. The Lindenmann's rule melting curve (L in Fig. 2) is in good agreement with the 34 ± 4 K/

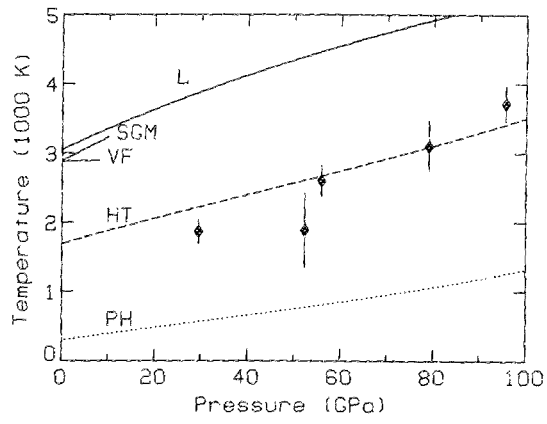

FIG. 2. Mo phase diagram. Calculations based on our data are represented by diamond symbols with 1σ error bars. The curves are: (L) Lindemann's rule melting curve calculation, (VF) experimental melting curve to 8 GPa of Vereshchagin and Fateeva (Ref. 19), (SGM) Clausius–Clapeyron melting slope measured by Shaner and co-workers (Ref. 18), (PH) calculated curve for the principal Hugoniot, and (HT) calculation for the 1400 °C Hugoniot. These curves were calculated with $q = 1$.

GPa slope of the fusion (SGM) determined by Shaner, Gathers, and Minichino.[18] The Lindemann's rule curve differs sizably, however, from the experimental measurements (VF) of Vereshchagin and Fateeva[19] to 8 GPa. Although these calculations are sensitive to q, the conclusion that our shock states are all within the field of solid stability is firm for q as high as three.

Further evidence that our samples remained solid is provided by the measurement of the bulk modulus from the shock data. As shown in the next section, the isentropic bulk modulus of 1400 °C Mo is between 225 and 244 GPa. This is similar to the room-temperature value of 261 GPa for solid Mo which we calculate from the principal Hugoniot data.[8] If the samples melted, the bulk modulus could be expected to drop by as much as a factor of 2.[20] The small drop in bulk modulus suggests that the samples remained solid.

B. Equation of state

The shock wave data for hot Mo, tabulated in Table I, were analyzed with a Eulerian finite strain expansion model[21] adapted for Hugoniot data analysis.[22–24] With this model, P-V data along a Hugoniot is mapped into a strain (f)—normalized isentropic pressure (F) plane, wherein the finite strain expansion for pressure may be linearized. This method of analysis is equivalent to fitting the P-V data (corrected to an isentrope) to the Birch–Murnaghan EOS. This transformation is accomplished by

$$f = [(V_0/V)^{2/3} - 1]/2 \tag{8}$$

and

$$F_{HS} = \frac{1 - 0.5\gamma[R(1+2f)^{1.5} - 1]}{3f(1+2f)^{1.5}[1 + (2 - 1.5\gamma)f]} P_H, \tag{9}$$

where $R \equiv V_{00}/V_0$, and V_{00} is the actual initial volume of the sample including any porosity. The subscript HS designates that the Hugoniot state has been transformed into an isentrope by means of Eq. (9). The thermodynamic Grüneisen parameter is assumed to be a function of volume alone according to Eq. (1). In the absence of phase changes, F and f are related by

$$F_{HS} = K_{0S}(1 - 2\xi_S f_{3H} + 4\zeta_S f_{4H}^2 + \cdots), \tag{10}$$

where

$$f_{3H} = f[1 + (2 - \gamma)f]/[1 + (2 - 1.5\gamma)f], \tag{11}$$

$$f_{4H}^2 = f^2[1 + (2 - 0.75\gamma)f]/[1 + (2 - 1.5\gamma)f], \tag{12}$$

$$\xi_S = \tfrac{1}{4}(4 - K'_{0S}), \tag{13}$$

and

$$\zeta_S = \tfrac{1}{8}\left[K_{0S}K''_{0S} + K'_{0S}(K'_{0S} - 7) + \tfrac{143}{9}\right]. \tag{14}$$

K_{0S}, K'_{0S}, and K''_{0S} are the zero-pressure isentropic bulk modulus, and its first and second derivatives with respect to pressure at constant entropy. The subscript 0 designates the initial zero-pressure state. The bulk modulus and its derivatives are calculated by multiple linear regression[25] with Eq. (10). The independent variables are f_{3H} and f_{4H}^2, and the dependent variable is F_{HS}.

The experimental data are presented in the f-F plane in Fig. 3. The error and scatter of the data are exaggerated in the f-F projection, as noted by Birch.[21] These data were calculated with the assumption that $q = 1$, for reasons that will be explained later. Another common assumption for q is that $q = 0$, or $\gamma =$ constant.[26,27] These calculations are, however, insensitive to our assumed value of q; values from 0.0 to 10.0 do not change the results. Following Heinz and Jeanloz,[23] the least-squares fitting of the data to Eq. (10) uses weighting according to the 1σ rms experimental errors on the assumption that these errors are normally distributed, consequently the data point for shot No. 707, which has the greatest error, carries little weight in the fit.

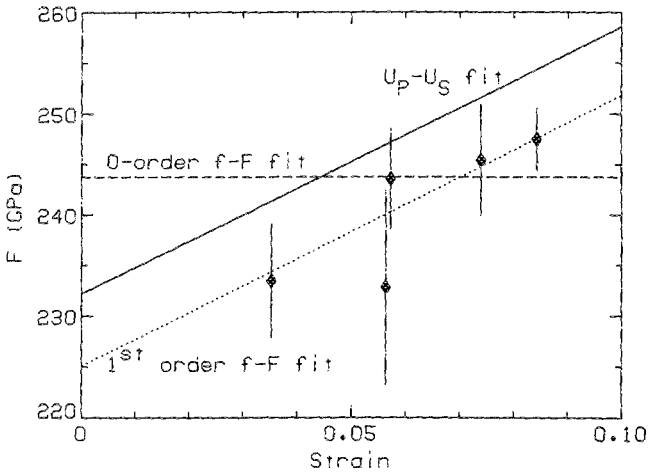

FIG. 3. Finite strain representation of the experimental data with 1σ errors. The f and F values were calculated with $q = 1$. Zero-order (dashed line) and first-order (dotted line) fits in the f-F plane are plotted with the fit from the U_P-U_S plane (solid line: see Fig. 4.).

A zero-order fit, or simple average (shown as the horizontal dashed line in Fig. 3), gives $K_{0S} = 244 \pm 2$ GPa and $K'_{0S} = 4$ and $K''_{0S} = -0.016$ GPa^{-1} from Eqs. (13) and (14), respectively. A first-order fit (shown as the dotted line in Fig. 3) gives $K_{0S} = 225 \pm 8$ GPa and $K'_{0S} = 4.76 \pm 0.33$. K''_{0S} is -0.023 GPa^{-1} from Eq. (14). Although the data are strongly suggestive of a linear relationship with positive slope, such a linear fit to our data is not statistically justifiable at a reasonable confidence level ($> 90\%$). In addition, it will be shown below that such a fit is not reconcilable with the 1-bar elasticity data on Mo.

An alternative method for calculating K_{0S} is to fit the data in the particle velocity (U_P)—shock velocity (U_S) plane.[5] Particle and shock velocities are related by

$$U_S = c_0 + sU_P, \tag{15}$$

where

$$c_0 = \sqrt{K_{0S}V_0} \tag{16}$$

and

$$s = \tfrac{1}{4}(1 + K'_{0S}). \tag{17}$$

The best fit to Eq. (15) is shown as the solid line in Fig. 4, and the values of K_{0S} and K'_{0S} determined from this fit are used in calculating the solid curve in Fig. 3. This fit gives $c_0 = 4.77 \pm 0.06$ km/s and $s = 1.43 \pm 0.5$, from which $K_{0S} = 232 \pm 6$ GPa and $K'_{0S} = 4.7 \pm 0.2$ are calculated.

These two calculations, although related,[28] are not interchangeable. A linear U_P-U_S relationship is identical to a first-order f-F fit only when[28] $18s\gamma_0 = 162s^2 - 360s + 215$; a condition which Mo fails to obey both on the principal Hugoniot and on the 1400 °C Hugoniot. The U_P-U_S fit is consistently offset from the f-F data in Fig. 3. For the purpose of calculating an impedance match the U_P-U_S fit is preferred. On the other hand, in calculating a Birch–Murnaghan isentrope, the f-F fit is preferred. These fits overlap within their 2σ errors.

These bulk modulus calculations may be compared with their cold counterparts computed from principal Hugoniot data.[8] These principal Hugoniot data are shown in the U_P-U_S and f-F projections in Figs. 4 and 5, respectively. Since no experimental errors are reported in Ref. 8, these data were fit without statistical weighting, i.e., with the assumption that all points have equal error. In Fig. 5 the U_P-U_S best-fit parameters are used in calculating the solid curves, and the zero- and first-order fits of the f-F data are plotted as the dashed and dotted curves, respectively. We calculate $K_{0S} = 261$ GPa and $K'_{0S} = 4$ from the zero-order f-F fit and $K_{0S} = 272$ GPa and $K'_{0S} = 3.71$ from the first-order f-F fit. The U_P-U_S fit gives $c_0 = 5.14$ km/s and $s = 1.22$ or $K_{0S} = 270$ GPa and $K'_{0S} = 3.88$. As with our data, only the zero-order fit of these data is statistically justifiable.

From a comparison of these data sets, we conclude that Mo is somewhat more compressible at higher temperatures. No firm conclusions may be drawn concerning its pressure derivative; however, the first-order fits would suggest that Mo becomes less compressible more rapidly at higher temperatures. This is consistent with our expectations since the two Hugoniot curves should be asymptotic at very high shock pressures.

These calculated moduli are independent of our assumptions regarding γ; that is, if we let $q = 0$, or $\gamma =$ constant, the resulting fit parameters do not vary within their error bars. Similarly, by neglecting the data of shot No. 707, which has anomalously high errors, the results are unchanged within the calculated errors.

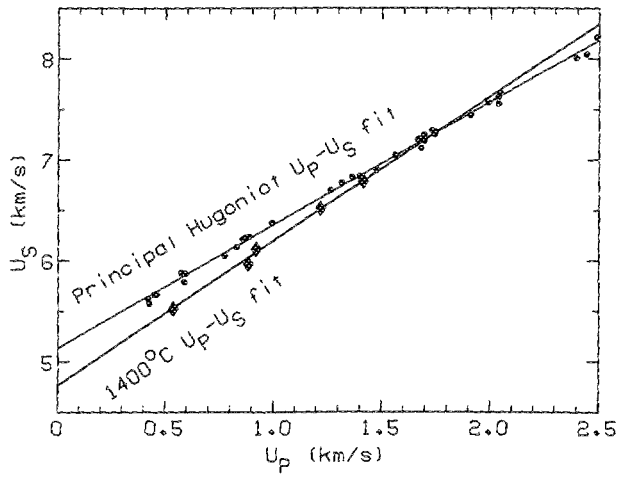

FIG. 4. Particle velocity vs shock velocity for Mo at 1400 °C (large diamond symbols) and 25 °C (small hexagonal symbols). The lines are least-squares best fits.

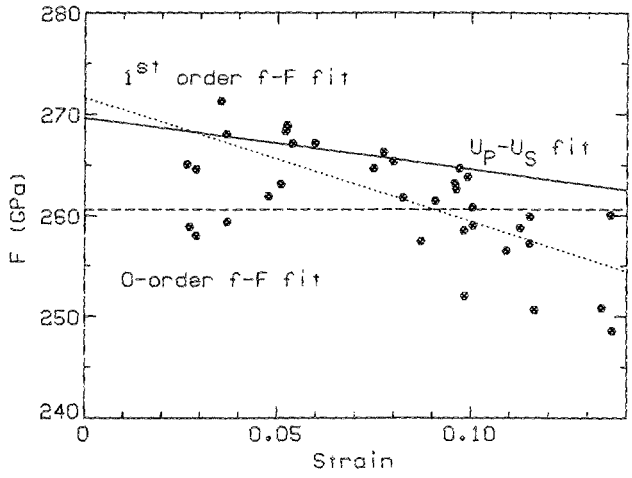

FIG. 5. Finite strain expansion representation of principal Hugoniot data in Marsh (Ref. 8). Zero-order (dashed line) and first-order (dotted line) fits in the f-F plane are plotted with the fit from the U_P-U_S plane (solid line; see Fig. 4).

C. Mie–Grüneisen equation of state

The experimental data may be compared with a thermodynamic model by computing the Hugoniot for a heated sample. The cold or principal Hugoniot, designated by subscript C, and the high-temperature Hugoniot, designated by subscript T, are related by the Mie–Grüneisen EOS at a constant shock volume, V_H by

$$P_{HT} = \left[P_{HC}\left(\frac{V_{0C} - V_H}{2} - \frac{V_H}{\gamma}\right) - \int_{T_{0C}}^{T_{0T}} C_P\, dT\right] \Big/ \left(\frac{V_{0T} - V_H}{2} - \frac{V_H}{\gamma}\right). \tag{18}$$

The initial volume of the preheated sample is calculated from its cold volume and the preheat temperature from the linear expansion data. Shock and particle velocities of the preheated samples may be calculated from

$$U_S = V_{0T}\sqrt{(P_{HT} - P_0)/(V_{0T} - V_H)} \tag{19}$$

and

$$U_P = \sqrt{(P_{HT} - P_0)(V_{0T} - V_H)}. \tag{20}$$

The cold Hugoniot P-V-U_P relationships are given by the shock EOS[5]

$$P_{HC} = (U_P/V_{0C})(c_0 + sU_P) \tag{21}$$

and

$$V_{HC} = [c_0 + (s-1)U_P]\, V_{0C}/(c_0 + sU_P), \tag{22}$$

where c_0, the zero-pressure sound speed, is given by Eq. (16), and s is given by Eq. (17).

The 1400 °C Hugoniot for Mo, calculated from Eqs. (16)–(22), is plotted in the V-P and U_P-P planes in Figs. 6 and 7, respectively. The calculated 1400 °C Hugoniot is also shown in the temperature-pressure plane in Fig. 2. For comparison, the principal Hugoniot is also plotted in Figs. 6 and 7. In these figures, the best fit 1400 °C Hugoniot is plotted as a thin solid curve, and the 1400 °C theoretical Mie–Grüneisen curve, with γ/V constant ($q = 1$) is plotted as a dashed line. The scatter of the data is significantly smaller in these projections than in the f-F projection. It is evident from these

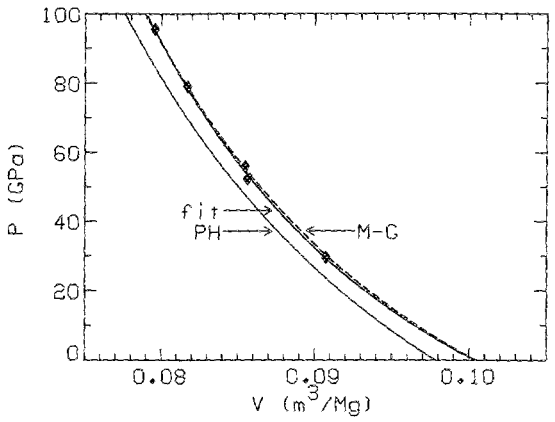

FIG. 6. 1400 °C Mo experimental data in the V-P plane. The curve labeled "fit" is calculated with the best fit U_P-U_S parameters. The "M-G" curve is calculated with the Mie–Grüneisen equation with $q = 1$. "PH" is the principal Hugoniot for comparison.

figures that the Mie–Grüneisen EOS models the experimental data quite well. The data refinement procedures of Rigden and co-workers,[3,4] which used this model to describe Mo as high T and P, are supported by our experiments.

Since Eq. (19) is sensitive to q, q may be used as a fit parameter to minimize the difference between the Mie–Grüneisen calculation and our experimental data. A value of $q \approx 1$ yields the best fit. We suggest therefore, that $q \approx 1$, and consequently that the Grüneisen parameter varies approximately in proportion to density. This agrees with the experimental determination[29] of $q \approx 1$ for Li, Na, and K.

D. Extrapolation of ultrasonic elasticity measurements

With q constrained to be ≈ 1, we may now employ a thermodynamic model of q to discriminate between our three model calculations of K_{0S} and K'_{0S}. Bassett *et al.*[26] derived the following thermodynamic expression for the parameter q:

$$q = 1 - \frac{(1+\gamma\alpha T)}{\alpha K_S}\frac{\partial K_S}{\partial T}\bigg|_P - \frac{\partial K_S}{\partial P}\bigg|_T + \gamma. \qquad (23)$$

The expression does not assume that γ is a function of volume alone, i.e., q is not required to be constant, but rather allows for a temperature dependence as well. More common formulations for γ assume γ to be a function of volume alone.[27,30] By way of the approximation $K'_{0S} \approx \partial K_S/\partial P|_T$,

$$\frac{\partial \ln K_{0S}}{\partial T}\bigg|_P = \frac{\alpha[1 - q - K'_{0S} + \gamma_0 (V/V_0)^q]}{1 + \alpha T \gamma_0 (V/V_0)^q}, \qquad (24)$$

the isentropic bulk modulus may be calculated as a function of temperature for an assumed constant value of q. V and α are both temperature-dependent quantities, thus Eq. (24) must be numerically integrated. Volume is calculated directly from the thermal expansion data in Table I, and the volumetric coefficient of thermal expansion, $\alpha \equiv \partial \ln V/\partial T|_P$, is calculated from the linear expansion relationships by

$$\alpha = 3\frac{\partial}{\partial T}\ln\left(1 + \frac{\Delta L}{L_0}\right)\bigg|_P. \qquad (25)$$

K'_{0S} is not known as a function of temperature, however, the zero-order f-F fits of both the principal and 1400 °C Hugoniot data suggest that $K'_{0S} \approx 4$, and is therefore independent of temperature. Although not statistically significant, the first-order f-F fits (dotted lines of Figs. 3 and 5) suggest that K'_{0S} (25 °C) < 4 and K'_{0S} (1400 °C) > 4, thus by approximating $K'_{0S} = 4$ Eq. (24) may overestimate K_{0S} at a given temperature. For simplicity we use the approximation $K'_{0S} = 4$ in Eq. (24).

Figure 8 shows a compilation of elasticity data for K_{0S} to 973 °C. Our three candidate values of K_{0S} at 1673 K are also included. The diamond symbols represent the values of K_{0S} calculated from the U_P-U_S best fit and the zero- and first-order f-F fits of our data. The data of Featherstone and Neighbours,[31] triangles in Fig. 8, are believed to be erroneous because of impurities in their samples.[32] The more recent data of Dickinson and Armstrong[33] are favored over the earlier data of Bolef and Klerk[34] for our calculations. The principal Hugoniot data reported by Marsh,[8] the hexagonal symbol, are in accord with the elasticity data of Dickinson and Armstrong. The value was calculated from the zero-order fit of the principal Hugoniot data in the f-F projection.

Equation (24) provides a functional form upon which

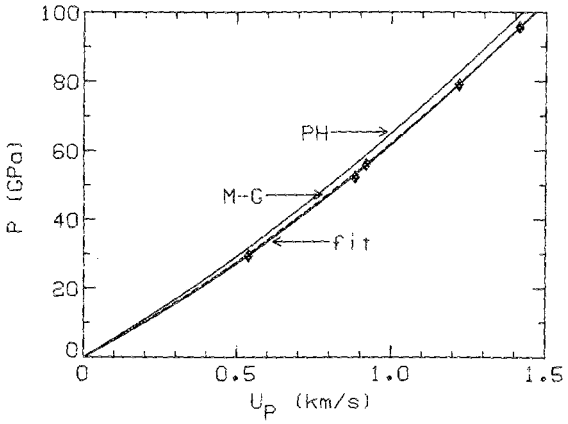

FIG. 7. 1400 °C Mo experimental data in the U_P-P plane. Labels correspond to Fig. 6.

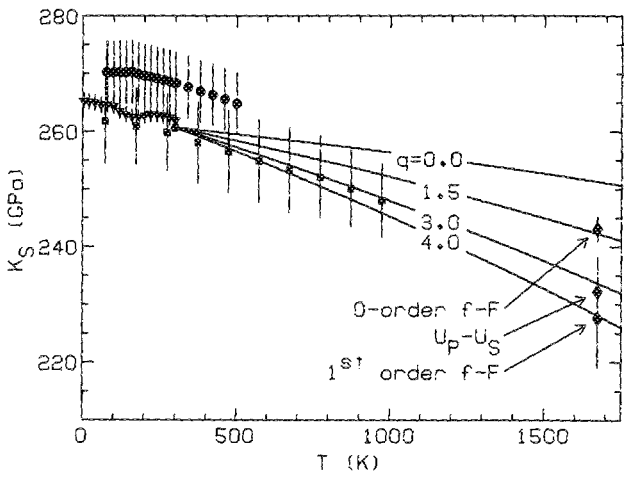

FIG. 8. Ultrasonic bulk modulus measurements and high-temperature shock moduli. Triangles, squares, and circles denote the elasticity values of Refs. 32, 33, and 34, respectively. The hexagonal symbol is calculated from the principal Hugoniot data in Marsh (Ref. 8) as the average F value in Fig. 5. The diamond symbols designate the various interpretations of the 1400 °C shock data. The solid curves are calculated with Eq. (24) for constant values of q from 1 to 4 using the value based on the principal Hugoniot data as a reference point.

to extrapolate the elasticity data to 1400 °C. Integration of Eq. (24) requires a single reference datum. We use the K_{0S} point derived from the principal Hugoniot data because it is in good agreement with the elasticity data, and because it was computed in the same manner as our datum.

Curves of constant q, calculated with Eq. (24), are plotted in Fig. 8. Within reported errors, q values from 1 to 5 satisfy the elasticity measurements of Dickinson and Armstrong. Because curves of constant q satisfy the data within their reported errors, no temperature dependence in the Grüneisen parameter is indicated except through the temperature dependence of V. A curve of $q = 1.5$ fits the elasticity data within their reported errors and agrees with our zero-order f-F fit datum. The $q = 4.0$ curve also falls within the errors of the elasticity data and agrees with the first-order datum. Our U_P-U_S determination falls near $q = 3.0$.

Since we suggested earlier that $q \approx 1$, we conclude based on Fig. 8 that only the zero-order fit of Fig. 3 can lead to an internally consistent view of the behavior of Mo initially heated to 1400 °C. The other fits presented in Fig. 3 would, in order to be consistent with the ultrasonic and principal Hugoniot data, require much higher values of q, which would lead to significant deviations between the calculated experimental temperatures and calculated Hugoniot temperature in the P-T plane (Fig. 2). Our best choices for K_{0S} and K'_{0S} are thus 244 ± 2 GPa and 4. We note that although Mo becomes more compressible at higher temperatures, it is less compressible than would have been predicted on the basis of linear extrapolation of the ultrasonic elasticity measurements alone.

We note, however, that this discrimination by q values is ambiguous when 2σ errors are allowed, that is all of the three candidates K_{0S} and K'_{0S} values overlap with 2σ error bars. This worst case uncertainty amounts to only about 5% uncertainty in K_{0S}, and 10% uncertainty in K'_{0S}.

Although the U_P-U_S best fit determination is not consistent with $q = 1$ [i.e., as shown in Fig. 8, if K_{0S} (1400 °C) = 232 GPa, then $q \approx 3$], it is nevertheless best for the purpose of calculating an impedance match.

IV. CONCLUSIONS

(1) New data on the dynamic compression of preheated molybdenum are presented. A zero-order fit to the finite strain model indicates a bulk modulus K_{0S} of 244 ± 2 GPa, and its pressure derivative K'_{0S} of 4 at 1400 °C. Higher order fits give values of K'_{0S} greater than 4, and are consistent with the finite strain expansion analysis, but are not statistically significant and are inconsistent with extrapolation of the ultrasonic data. The temperature derivative of K_{0S} at zero pressure is thus approximately -0.012 GPa/K. The Hugoniot parameters for Mo at 1400 °C are $c_0 = 4.77 \pm 0.06$ km/s and $s = 1.43 \pm 0.05$.

(2) The Mie–Grüneisen EOS has been demonstrated to be a good model for the shock behavior of Mo at high temperatures.

(3) Our data suggest that the Grüneisen parameter is proportional to density, and no evidence is found for a temperature dependence in γ. If this suggestion is correct, the zero-order fit to the finite strain model is favored.

ACKNOWLEDGMENTS

We thank M. Long and E. Gelle for their expert technical assistance with the preparation and execution of the shock experiments. L. Young polished some of the Mo samples. Discussion and review by D. J. Stevenson was very helpful. We appreciate the use of the 10 kW rf heater provided by L. T. Silver. This work was funded by NSF Grant Nos. EAR-86-18545 and EAR-85-08969. Contribution number 4510, Division of Geological and Planetary Sciences, California Institute of Technology, CA.

[1] H. K. Mao, P. M. Bell, J. W. Shaner, and D. J. Steinberg, J. Appl. Phys. **49**, 3276 (1978).
[2] C. E. Regan III, M. B. Silbert, and B. C. Diven, J. Appl. Phys. **48**, 2860 (1977).
[3] S. M. Rigden, T. J. Ahrens, and E. M. Stolper, J. Geophys. Res. (1987) (in press).
[4] S. M. Rigden, T. J. Ahrens, and E. M. Stolper, Science **226**, 1071 (1984).
[5] T. J. Ahrens, in *Methods of Experimental Physics*, edited by C. G. Sammis and T. L. Henyey (Academic, New York, 1987), Vol. 24, p. 185.
[6] F. Birch, J. Geophys. Res. **57**, 227 (1952).
[7] S. P. McQueen, memo of May 1, 1969.
[8] S. P. Marsh, *LASL Shock Hugoniot Data* (University of California Press, Berkeley, 1980).
[9] M. E. Straumanis and R. P. Shodman, Z. Metallkd. **59**, 492 (1968).
[10] Y. S. Touloukian, R. K. Kirby, R. E. Taylor, and P. D. Desai, *Thermal Expansion of Metallic Elements and Alloys* (Plenum, New York, 1970).
[11] S. P. McQueen, S. P. Marsh, J. W. Taylor, J. N. Fritz, and W. J. Carter, in *High Pressure Impact Phenomena*, edited by R. Kinslow (Academic, New York, 1970), p. 293.
[12] R. A. Robie, B. S. Hemingway, and J. R. Fisher, *Thermodynamic Properties of Minerals and Related Substances* (U. S. Geol. Survey Bull. 1452, Washington, DC, 1978).
[13] S. Eliezer, A Ghatak, and H. Hora, *An Introduction to Equations of State: Theory and Applications* (Cambridge University Press, New York, 1986).
[14] T. J. Ahrens, J. Geophys. Res. **84**, 985 (1979).
[15] J. J. Gilvarry, Phys. Rev. **102**, 317 (1956).
[16] M. Hoch, *Thermodynamic Nuclear Materials Proceedings of the Fourth Symposium 1974* (International Atomic Energy Association, Vienna, 1975), Vol. 2, p. 113.
[17] R. Hultgren, R. L. Orr, P. D. Anderson, and K. K. Kelley, *Selected Thermodynamic Properties of Metals and Alloys* (Wiley, New York, 1963).
[18] J. W. Shaner, G. R. Gathers, and C. Minichino, High Temp.-High Press. **9**, 331 (1977).
[19] L. F. Vereshchagin and N. S. Fateeva, High Temp.-High Press. **9**, 619 (1977).
[20] B. Kamb, in *Structural Chemistry and Molecular Biology*, edited by A. Rich and N. Davidson (Freeman, San Francisco, 1968), p. 507.
[21] F. Birch, J. Geophys Res. **83**, 1257 (1978).
[22] R. Jeanloz and T. J. Ahrens, Geophys. J. R. Aston. Soc. **62**, 505 (1980).
[23] D. L. Heinz and R. Jeanloz, J. Appl. Phys. **55**, 885 (1984).
[24] T. J. Ahrens and R. Jeanloz, J. Geophys. Res. **92**, 10363 (1987).
[25] W. H. Press, B. P. Flannery, S. A. Teukolsky, and W. T. Vetterling, *Numerical Recipes* (Cambridge University Press, New York, 1986).
[26] W. A. Bassett, T. Takahashi, H. Mao, and J. S. Weaver, J. Appl. Phys. **39**, 319 (1968).
[27] D. L. Anderson, Phys. Earth Planet. Inter. **45**, 307 (1987).
[28] R. Jeanloz and R. Grover, in *Proceedings of the American Physical Society Topical Conference on Shock Waves in Condensed Matter*, Monterey, CA, 20–23 July, 1987, edited by S. C. Schmidt and N. C. Holmes (Plenum, New York, 1987) (in press).
[29] R. Boehler, Phys. Rev. B **27**, 6754 (1983).
[30] D. L. Anderson, Geophys. J. R. Astron. Soc. **13**, 9 (1967).
[31] F. H. Featherstone and J. R. Neighbours, Phys. Rev. **130**, 1324 (1963).
[32] L. Berg. G. Czack, E. Koch, and J. Wagner, *Gmelin Handbook of Inorganic Chemistry, 8th Edition, Molybdenum Supplemental Volume A 2a* (Springer, New York, 1985), p. 379.
[33] J. M. Dickinson and P. E. Armstrong, J. Appl. Phys. **38**, 602 (1967).
[34] D. I. Bolef and J. de Klerk, J. Appl. Phys. **33**, 2311 (1962).